A Stopped-Flow Kinetic Study of the Solubilization of Acridine Orange and Its 10-Alkyl Derivatives into the Micelle of Sodium Dodecyl Sulfate

Yukio KUBOTA,* Naofumi OMURA, and Kiyofumi MURAKAMI
Department of Chemistry, Faculty of Science, Yamaguchi University, Yamaguchi 753
(Received August 27, 1990)

Stopped-flow method has been used to investigate the kinetics of the solubilization of Acridine Orange (AO, 3,6-bis(dimethylamino)acridinium chloride) and its 10-alkyl derivatives into the micelle of sodium dodecyl sulfate (SDS). The reaction curves of the SDS–AO and SDS–10-alkyl AO systems were characterized by single and double exponential functions, respectively. It was found that all the time constants are concentration dependent and approach limiting values at high reactant concentrations. The data were fitted by a minimal mechanism in which a rapid bimolecular step is followed by one (AO) or two (10-alkyl derivatives of AO) sequential isomerizations. All the rate constants determined for this mechanism markedly decrease with an increase in the length of the introduced alkyl chain. The equilibrium constants for the bimolecular and first isomerization steps do not highly depend on the size of the alkyl chain, while the equilibrium constant for the second isomerization step progressively increases with increasing it. The spectral changes with time indicate that the bound dye gradually migrates to more hydrophobic environment inside the micelle. These results lead to the conclusion that the steps in the proposed mechanism correspond to rapid adsorption of the dye to the micelle surface site, followed by reorientation of the dye and then migration of its alkyl chain into the hydrophobic region of the micelle.

The most important properties of micellar systems are their ability to solubilize a variety of molecules and their catalytic effects on many reactions occurring at the micelle surface and inside.[1–3] In order to better understand the nature of this solubilization and the physicochemical behavior of solubilized molecules, it is of fundamental significance to obtain information concerning the structure of micelles and the location or relative orientation of solubilized molecules.[4,5] For this purpose, several spectroscopic techniques such as NMR,[6,7] ESR,[8] and fluorescence[9–13] have been employed so far.

Kinetic methods, though helpful in understanding the solubilization mechanism, have rarely been applied to the solubilization phenomena.[14–19] Robinson and co-workers[16,17] proposed a mechanism in which rapid adsorption of dye on the micelle surface is followed by slow penetration into the hydrocarbon interior of the micelle. On the other hand, Takeda et al.[14] proposed the rapid initial formation of a dye-surfactant salt which then penetrates the palisade layer of the micelle. However, there is no extensive discussion based on the evaluation of equilibrium and rate constants for each step.

This paper describes detailed results on the kinetics of the solubilization of Acridine Orange (AO) and its 10-alkyl derivatives into the micelle of sodium dodecyl sulfate (SDS), studied by stopped-flow method with absorption and fluorescence detection. The aim of the present study is to establish the mechanism of the solubilization through the evaluation of equilibrium and rate constants. Among the results, it is revealed that the solubilization process consists of rapid initial adsorption of the dye on the micelle surface and one (AO) or two subsequent isomerizations (10-alkyl derivatives of AO).

Experimental

AO (3,6-bis(dimethylamino)acridinium chloride) was purchased from Merck. The 10-alkyl derivatives of AO (methyl-AO, propyl-AO, pentyl-AO, octyl-AO, and decyl-AO) were synthesized according to the method of Miethke and Zanker.[20] All dyes were purified by repeated recrystallizations and column chromatography; no trace of impurity was detected by the method of thin-layer chromatography for each dye. SDS (specially pure grade >99%) was obtained from Nakarai Chemicals and used without further purification. All other chemicals were reagent grade and deionized redistilled water was used for the preparation of all aqueous solutions.

Absorption and fluorescence spectra were measured with a Shimadzu UV-200S spectrophotometer and a Hitachi MPF-2A fluorescence spectrophotometer, respectively. The critical micelle concentration (cmc) of SDS in the absence and presence of dye was determined by the conductometric method. Kinetic measurements were made on a Union Giken RA-601 rapid-scanning stopped-flow spectrophotometer using both absorbance and fluorescence detection, a 1:1 mixing ratio, and a 2 mm path-length cell. The dead time of the instrument was 0.6 ms, as judged from the reduction reactions of 2,6-dichloroindophenol by L-ascorbic acid.[21] In the kinetic experiments, the initial concentration of SDS was always maintained in large excess of that of the dye. The resulting reaction curves were subjected to multiexponential analysis with a nonlinear least-squares regression program based on the Marquardt algorithm.[22] All measurements were carried out at 25±0.2 °C.

All the calculations were accomplished with an Acos-850 computer system (NEC Corporation) and/or a PDP 11 minicomputer (Digital Equipment Corporation).

Results and Discussion

Electronic Spectra and CMC. The alkyl derivatives of AO when mixed with SDS solutions showed absorp-

tion and fluorescence changes similar to those reported for AO.[16,17,23] Figure 1 displays typical absorption spectra obtained with pentyl-AO (1.0×10^{-5} M) in the presence of SDS. The spectra are characterized by two absorption bands; one is the monomer band at 495 nm and the other (470 nm) is the band due to the dimer or higher aggregates.[16,23] Below the cmc, the spectrum of pentyl-AO exhibits both a reduction of the band at 495 nm and an enhancement of the band at 470 nm with increasing SDS concentration. This behavior is ascribed to the ion pair (or salt) formation between the dye cation and the SDS anion, followed by the formation of mutual induced aggregates. In the vicinity of the cmc, the monomer band markedly increases and then the shape of spectrum remains unchanged above the cmc. The absorption maximum above the cmc shifts toward longer wavelengths compared to that of free dye in aqueous solutions (492 nm). The fluorescence quenching of the dye below the cmc and the strong enhancement of its fluorescence above the cmc were observed for all dyes; above the cmc, a blue shift and a narrowing of the fluorescence band were also observed when compared to that of free dye in aqueous solutions. These absorption and fluorescence properties above the cmc suggest that the dye is solubilized in a hydrophobic region of the micelle and exists as a monomeric form.[9,16,23]

The cmc of SDS solution, in agreement of the literature value,[24] was 8.0×10^{-3} M (1 M=1 mol dm^{-3}) and the presence of dye (1.0×10^{-5} M) had no appreciable influence on cmc irrespective of the dye structure.

Kinetics of Solubilization. It is well-known that AO and its alkyl derivatives aggregate in aqueous solutions at higher concentrations.[17,25,26] To minimize the effect of dye aggregation, kinetic measurements were made on solutions in which dye concentrations were kept below 10^{-5} M; in fact, the kinetic behavior was idependent of dye concentrations in the range of 2.5×10^{-6} to 2.0×10^{-5} M. Figure 2 displays typical time courses of absorbance changes after mixing an equal volume of AO and SDS solutions (curve a) and of pentyl-AO and SDS solutions (curve b). The reaction curve of the AO–SDS system was characterized by a single-exponential function, while that of the pentyl-AO–SDS system by a double-exponential one. Figures 3 and 4 show the dependence of the reciprocal of the time constant (τ^{-1}; apparent rate constant) on [SDS]—cmc for the AO–SDS and pentyl-AO–SDS systems respectively; here, [SDS] stands for the total SDS concentration. It can be seen that τ^{-1} increases with an increase in the SDS concentration and reaches a

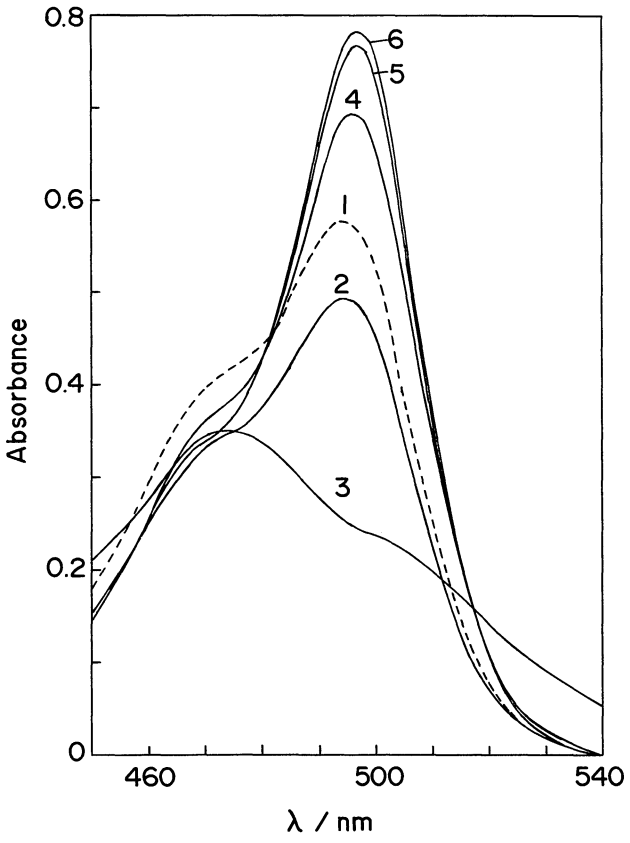

Fig. 1. Absorption spectra of pentyl-AO (1.0×10^{-5} M) in the presence of various concentrations of SDS at 25 °C. [SDS]/M: (1) 0; (2) 1.0×10^{-5}; (3) 2.0×10^{-3}; (4) 6.0×10^{-3}; (5) 8.0×10^{-3}; (6) 2.0×10^{-2}.

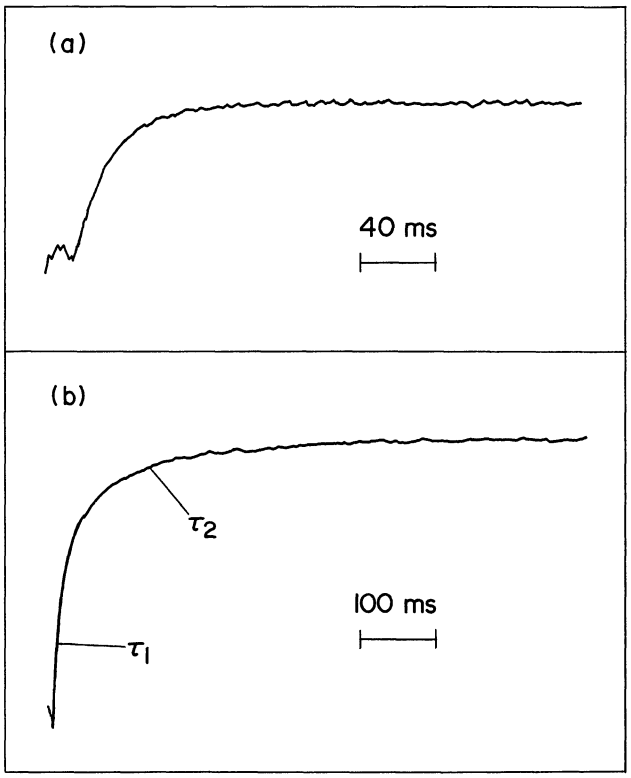

Fig. 2. Typical time courses of absorbance changes observed at 498 nm after mixing of (a) [AO]=2.0×10^{-5} M and [SDS]=5.0×10^{-2} M and (b) [pentyl-AO]=2.0×10^{-5} M and [SDS]=4.0×10^{-2} M.

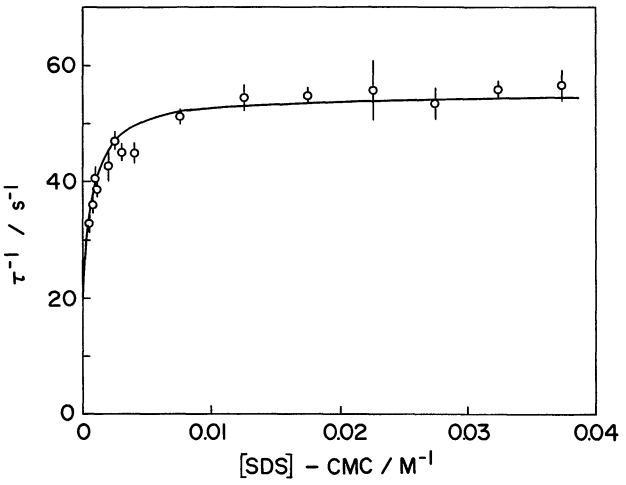

Fig. 3. Dependence of τ^{-1} on [SDS]—cmc for the AO–SDS system. The concentration of AO was 1.0×10^{-5} M. The line is drawn using Eq. 4 with parameters listed in Table 1.

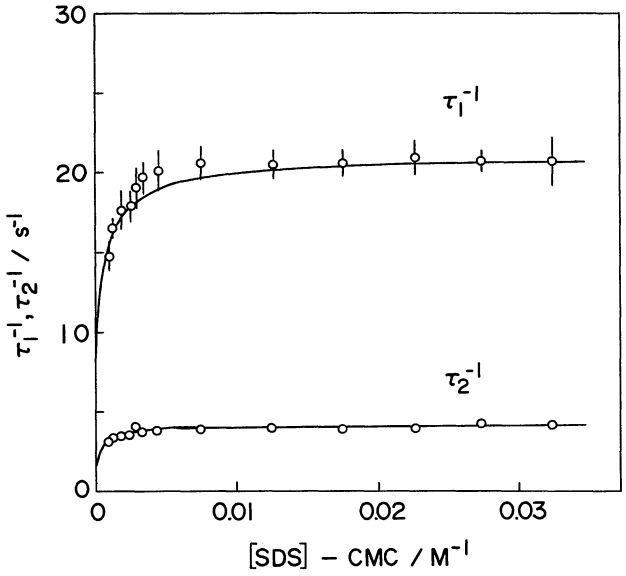

Fig. 4. Dependence of τ_1^{-1} and τ_2^{-1} on [SDS]—cmc for the pentyl-AO–SDS system. The concentration of pentyl-AO was 1.0×10^{-5} M. The lines are drawn using Eq. 5 with parameters listed in Table 1.

limiting value (Figs. 3 and 4). The reaction of SDS with propyl-AO or decyl-AO was also examined with fluorescence detection. As Fig. 5 shows the result obtained with the decyl-AO–SDS system, the time constants determined from absorbance and fluorescence changes agree well with each other. This implies that absorbance and fluorescence changes reflect the same reaction process. In the case of octyl-AO or decyl-AO, additional rapid changes in both the absorbance and the fluorescence intensity were observed. Their magnitudes, however, were too small to

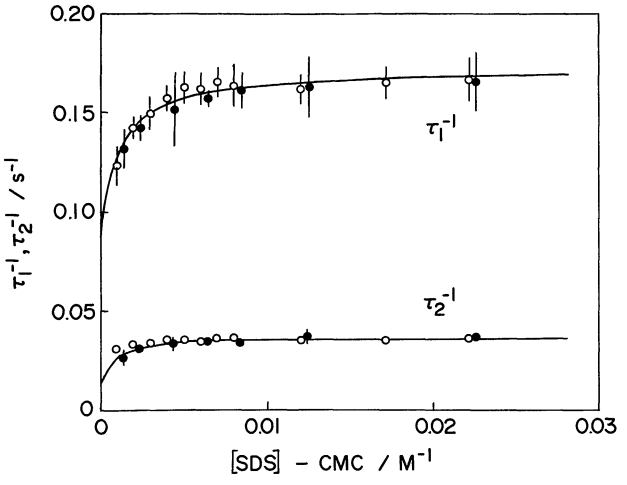

Fig. 5. Dependence of τ_1^{-1} and τ_2^{-1} on [SDS]—cmc for the decyl-AO–SDS system: (○) absorbance detection; (●) fluorescence detection. The concentration of decyl-AO was 1.0×10^{-5} M for absorbance detection and 5.0×10^{-6}M for fluorescence detection. The lines are drawn using Eq. 5 with parameters listed in Table 1.

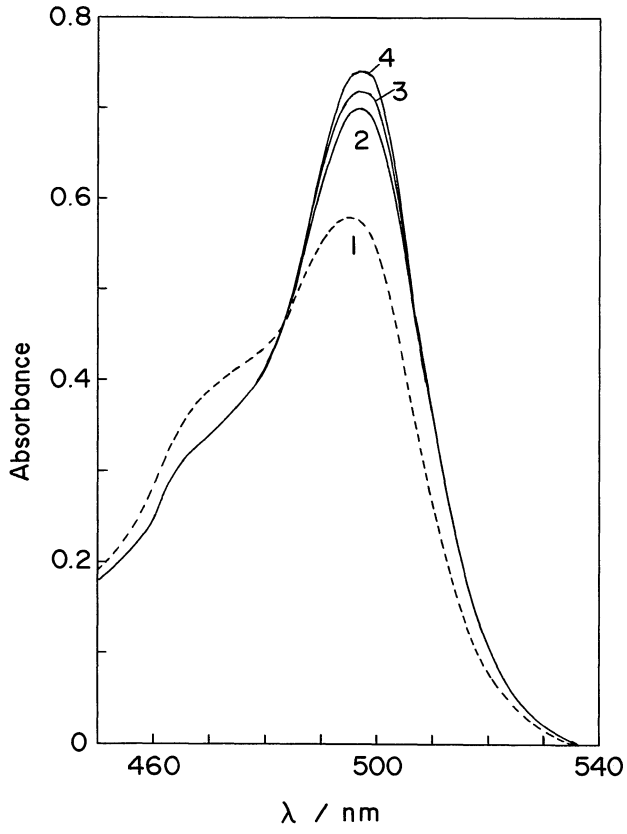

Fig. 6. Spectral change of pentyl-AO (1.0×10^{-5} M) after mixing with SDS (2.0×0^{-2} M). (1) spectrum of pentyl-AO in the absence of SDS; (2) t=12.5 ms; (3) t=32.5 ms; (4) t=152.5 ms. t denotes the time after mixing.

determine the accurate time constant.

To see the time course of spectral changes in the solubilization process, stopped-flow rapid scanning spectroscopy was employed. Figure 6 depicts a typical result obtained with the pentyl-AO–SDS system. It can be seen that the absorbance at the monomer band increases and the absorption maximum shifts toward a longer wavelength with time. This result supports that the dye is solubilized into the hydrophobic environment of the micelle in a monomeric form.[9,16,23]

Mechanism of Solubilization. Some mechanisms for the solubilization of dye into the surfactant micelle have been proposed. Hoffmann[15] suggested that the rapid formation of a dye-surfactant ion pair is followed by a stepwise accumulation of surfactant monomers around the ion pair until a dye-containing micelle is built up. Robinson and co-workers[16,17] observed that the reaction curve for the 10-alkyl AO–SDS system is approximately characterized by a single-exponential function and the first-order rate constant markedly decreases with increasing the size of the alkyl chain. Their observation argues against the suggestion of Hoffmann,[15] that the micelle breakdown is the rate-determining step, since such a process should be fast and independent of the dye structure. Therefore, they proposed another mechanism in which rapid adsorption of the dye on the micelle surface is followed by slow penetration of the dye into the hydrophobic region of the micelle;[16,17] the concentration dependence of the rate constant was consistent with that expected for the slow step.

The results obtained in this study clearly indicate that the reaction of SDS with AO is characterized by one time constant, whereas the reactions of SDS with 10-alkyl derivatives of AO by two time constants. The latter finding is distinguishable from that of Robinson et al.[17] To interpret the present data, we propose the following schemes for the solubilization of the dye into the surfactant micelle: for AO,[16]

$$\mathrm{D} + \mathrm{M} \underset{k_{-2}}{\overset{K_1}{\rightleftharpoons}} \mathrm{DM}_1 \underset{}{\overset{k_2}{\rightleftharpoons}} \mathrm{DM}_2, \qquad (1)$$

and for 10-alkyl derivatives of AO,

$$\mathrm{D} + \mathrm{M} \underset{k_{-2}}{\overset{K_1}{\rightleftharpoons}} \mathrm{DM}_1 \underset{k_{-3}}{\overset{k_2}{\rightleftharpoons}} \mathrm{DM}_2 \underset{}{\overset{k_3}{\rightleftharpoons}} \mathrm{DM}_3, \qquad (2)$$

where D, M, and DM_i denote the dye, the micelle surface site and the i-th dye-surfactant complex, respectively, and K_i, k_i, and k_{-i} are equilibrium, forward rate and backward rate constants for the i-th step, respectively. The first step can be assigned to the adsorption of the dye on the micelle surface and the subsequent ones to the isomerizations of the complexes. Since the initial binding of the dye to the micelle is considered to be electrostatic in nature and there is no restriction of a single site on each micelle, the concentration of the micelle surface site ([M]) can be defined as[16]

$$[\mathrm{M}] = \alpha([\mathrm{SDS}] - \mathrm{cmc}), \qquad (3)$$

where α is the fraction of micelle surface charge which is not neutralized by Na^+ counterion; the value of α was evaluated to be 0.168 by dividing the surface charge of the SDS micelle by its association number.[27] On the assumption that the bimolecular adsorption step is faster than the isomerization step and [M]>>[D], the time constant for the second step in Scheme 1 is simply expressed by[28]

$$\tau^{-1} = k_2K_1[\mathrm{M}]/(1 + K_1[\mathrm{M}]) + k_{-2}. \qquad (4)$$

To secure the requirement [M]>>[D], experimental conditions were regulated in such a way that there is always an excess of micelle sites. Under these conditions the possible complication due to dye–dye interactions on the micelle surface is eliminated.

Estimating the starting values from the intercept and initial slope of a plot of τ^{-1} versus [M] and from the plateau value of τ^{-1}, kinetic parameters (K_1, k_2, and k_{-2}) were determined by a nonlinear regression analysis so as to fit the expression of τ^{-1} (Eq. 4) to the observed data.[22] The results are summarized in Table 1. It is found that the k_2 value for AO (40 s^{-1}) is very similar to the value (47.6 s^{-1}) reported by Robinson et

Table 1. Equilibrium and Rate Constants at 25 °C

Dyes	K_1 / $M^{-1}\times10^{-3}$	K_2	k_2 / s^{-1}	k_{-2} / s^{-1}	K_3	k_3 / s^{-1}	k_{-3} / s^{-1}	K_T / $M^{-1}\times10^{-4}$
AO	11	2.6	40	15				3.8
Methyl-AO	9.5	1.8	79	43	1.9	65	35	6.0
Propyl-AO	11	1.7	41	24	4.2	29	7.0	11
Pentyl-AO	12	2.5	14	5.6	5.1	4.6	0.89	19
Octyl-AO	12	2.5	0.75	0.30	6.1	0.27	0.044	22
Decyl-AO	5.8	2.3	0.11	0.047	12	0.049	0.004	18

al.[16]

For the 10-alkyl AO–SDS systems (Scheme 2), the time constants for the two isomerization steps can be expressed by[28]

$$\tau_1^{-1},\ \tau_2^{-1} = \frac{1}{2}[(a_{11}+a_{22}) \pm \{(a_{11}-a_{22})^2 + 4a_{12}a_{21}\}^{1/2}], \quad (5)$$

where

$$a_{11} = k_2K_1[\mathrm{M}]/(1+K_1[\mathrm{M}]) + k_{-2} + k_3, \quad (6)$$

$$a_{12} = k_2K_1[\mathrm{M}]/(1+K_1[\mathrm{M}]) - k_{-3}, \quad (7)$$

$$a_{21} = -k_3, \quad (8)$$

$$a_{22} = k_3. \quad (9)$$

It should be noted that Eq. 5, as in the case of Eq. 4, holds on the assumption [M]≫[D] which is the case in this study. Equation 5 is a complex expression, but the problem can easily be solved by considering the following expressions:

$$\tau_1^{-1}\cdot\tau_2^{-1} = (k_3+k_{-3})(\tau_1^{-1}+\tau_2^{-1}) - (k_3+k_{-3})k_2 - k_{-2}k_{-3}, \quad (10)$$

$$\tau_1^{-1}+\tau_2^{-1} = k_2K_1[\mathrm{M}]/(1+K_1[\mathrm{M}]) + k_{-2} + k_3 + k_{-3}. \quad (11)$$

In the same manner as Eq. 4, the curve-fitting analysis of Eq. 11 gives K_1, k_2, and $k_{-2}+k_3+k_{-3}$. Then, the values of k_{-2}, k_3 and k_{-3} are determined from the slope and intercept of a plot of $\tau_1^{-1}\cdot\tau_2^{-1}$ against $(\tau_1^{-1}+\tau_2^{-1})$. The kinetic parameters thus obtained are listed in Table 1. The solid lines in Figs. 3—5 represent the theoretical ones calculated on the basis of kinetic parameters in Table 1; there is a satisfactory agreement between observed and calculated values.

Takeda et al.[14] found that when pinacyanol solution is mixed with the solution containing SDS micelles, the absorption band characteristic of the surfactant-dye salt appears and this is progressively replaced by the monomer band of the dye with time. To interpret the kinetics of the solubilization of pinacyanol into the SDS micelle, they proposed the rapid initial formation of the salt which then penetrates the palisade layer of the micelle.[14] A similar mechanism was also suggested for the solubilization of an anthraquinone acidic dye into the micelle of hexadecyltrimethylammonium bromide (HTAB).[19] Since hydrophobic interactions between hydrocarbon chain attached to AO and surfactant stabilize the salt, it is expected that the salt formation might be pronounced with an increase in the length of the alkyl chain. In the present systems, unambiguous evidence for the salt formation was not obtained from both the rapid-scanning spectroscopy (Fig. 6) and the wavelength dependence of optical changes in reaction curves. Nevertheless, it seems worthwhile to examine some possibility of the salt formation, since this is anticipated to be a very rapid process outside the time range of stopped-flow measurements. In such a case, the following kinetic scheme should be considered:

$$\mathrm{D} + x\mathrm{S} \overset{K_0}{\rightleftharpoons} \mathrm{DS}_x,$$

$$\mathrm{DS}_x + \mathrm{M} \overset{K_1}{\rightleftharpoons} \mathrm{DM}_1 \overset{K_2}{\rightleftharpoons} \mathrm{DM}_2 \overset{K_3}{\rightleftharpoons} \mathrm{DM}_3. \quad (12)$$

In Scheme 12, S is the surfactant monomer, DS_x is the salt of dye with surfactant molecules, x is a small integer, and K_0 is the equilibrium constant for the salt formation. If we assume that both the salt formation and the adsorption of the salt on the micelle surface are rapid, we can find that the time constants for the isomerization steps are also expressed by Eq. 6. In the expressions for τ_1^{-1} and τ_2^{-1},

$$a_{11} = k_2K_1[\mathrm{M}]/\{(1+1/K_0[\mathrm{S}]^x) + K_1[\mathrm{M}]\} + k_{-2} + k_3, \quad (13)$$

$$a_{12} = k_2K_1[\mathrm{M}]/\{(1+1/K_0[\mathrm{S}]^x) + K_1[\mathrm{M}]\} + k_{-3}, \quad (14)$$

$$a_{21} = -k_3, \quad (15)$$

$$a_{22} = k_{-3}. \quad (16)$$

If the salt formation predominatly occurs, that is, $K_0[\mathrm{S}]^x \gg 1$, Eqs. 13—16 are reduced to Eqs. 6—9. In this case, two schemes (Scheme 2 and Scheme 12) can not kinetically be distinguished. Here, it should be noted that K_1 in Scheme 12 is the equilibrium constant for the adsorption of the salt (DS_x). Since D having a positive charge is more accessible to the negatively charged micelle surface than DS_x which is neutral or negatively charged, K_1 for DS_x (Scheme 12) is expected to be smaller than that for D (Scheme 2). Table 1 indicates that K_1 does not depend on the length of the alkyl chain except decyl-AO. This finding suggests that not hydrophobic but eletrostatic interactions make major contributions to the driving force for the adsorption process. The smaller value for decyl-AO is presumably a result of appreciable formation of the salt which leads to weakening the electrostatic force. Moreover, the additional rapid reaction observed for decyl-AO dye or octyl-AO may be attributed to the adsorption of the salt and/or to its dissociation on the micelle surface which takes place rapidly prior to the penetration of the dye into the micelle. In view of the considerations stated above, it seems reasonable to conclude that Scheme 2 prevails for the AO derivatives with shorter alkyl chains, whereas Scheme 12, in addition to Scheme 2, makes some contributions to the kinetics of the solubilization for the AO derivativs with longer alkyl chains.

K_2 has similar values for all dyes, whereas the

forward and backward rate constants of the second step (k_2 and k_{-2}) gradually decrease with increasing the length of the alkyl chain (Table 1). This result shows that the second step is not driven by hydrophobic force, but the alkyl chain plays an important role for the activation of the second step. One possible mechanism is the reorientation of the dye at the micelle surface which includes partial penetration of the alkyl chain through the surface layer of the micelle. This process must be accompanied by the release of hydrated water molecules surrounding the alkyl chain.[29] Therefore, the rate constants for the second step are expected to decrease with increasing the size of the alkyl chain.

Table 1 also indicates that both the equilibrium and the rate constants for the third step highly depend on the length of the alkyl chain; K_3 increases with increasing the size of the alkyl group, while k_3 and k_{-3} decrease. This result suggests that the final form of the complex is stabilized by the hydrophobic force. On the other hand, the spectral change of the dye with time (Fig. 6) obviously shows that the dye is solubilized into the hydrophobic environment. In view of these results, it seems reasonable to assign the third step to the migration of the alkyl chain from the micelle surface to the *inner* hydrophobic site of the micelle.

Figure 7 displays the standard free energy changes ($\Delta G_2°$, $\Delta G_3°$, $\Delta G_{2+3}°$) for the second and third steps in Schemes 1 and 2 as a function of the number of carbon atoms in the alkyl chain (n); $\Delta G_{2+3}°$ corresponds to the standard free energy changes for the overall isomerization process. The free energy of transfer of a methylene group to the inside of the micelle can be estimated

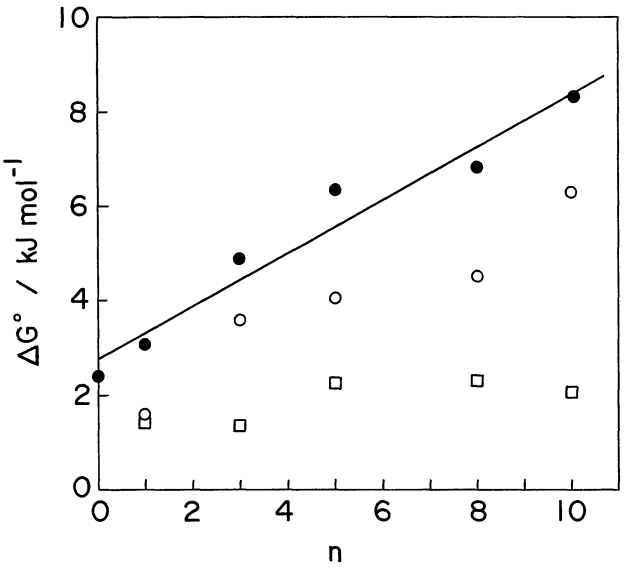

Fig. 7. The standard free energy changes for the isomerization steps as a function of the number of carbon atoms in the alkyl chain (n). (□) $\Delta G_2°$; (○) $\Delta G_3°$; (●) $\Delta G_{2+3}°$. The line is the least-squares fit for $\Delta G_{2+3}°$.

from the slope of a linear plot of $\Delta G_{2+3}°$ versus n;[29] the value was found to be about 0.6 kJ mol^{-1}. This value is about a half to one third of that estimated for the transfer of a hydrocarbon to the SDS micelle.[29] Possibly this smaller value of the free energy of transfer is due to the presence of the bulky acridine head group.

The overall binding constant K_T can be defined by

$$K_T = K_1(1 + K_2 + K_2K_3). \quad (17)$$

As shown in Table 1, the K_T values are the order of 10^4 to 10^5 M^{-1}. To confirm the mechanism of the solubilization, it is necessary to determine binding constants for micelles by means of other techniques. In spite of the desire to have useful, general methods for obtaining such constants, the present state of affairs remains difficult. Fluorescence techniques have been applied to evaluate rough binding constants, but their number is quite limited.[10,11,30] Chiang and Lukton[10] reported $K_T \approx 2\times10^3$ M^{-1} for the binding of 6-(*p*-toluidino)-2-naphthalenesulfonate to the SDS micelle. On the other hand, Reed et al.[11] estimated the following association constants of Rose Bengal binding to HTAB and SDS micelles; $K_T(\text{HTAB}) \geqq 10^4$ M^{-1} and $K_T(\text{SDS}) \geqq 10^2$ M^{-1}. By employing the fluorescence quenching method, Zoltewicz and Munoz[30] have recently reported that the association constants of heterocyclic cations such as 10-methylacridinium and ethidium bromide to the SDS micelle range between 1.0×10^4 and 1.4×10^5 M^{-1}. This method gives more accurate binding constants and its application to our systems will be an interesting subject. The above results suggest that the magnitude of K_T, when the charges of the dye and micelle are opposite, is much larger ($\geqq 10^4$—10^5 M^{-1}) compared to that ($\approx 10^3$ M^{-1}) with the same charge. It is worth noting that the K_T values in this study are to be expected for the binding of cationic dyes to the anionic micelle. As can be seen from Table 1, K_T increases with increasing the size of the alkyl chain except a somewhat smaller value for decyl-AO. This behavior can be understood in terms of the combined effect of the electrostatic interaction, which is responsible for K_1, and of the hydrophobic interaction, which predominantly affects K_3.

In conclusion, the stopped-flow kinetic study reveals that the solubilization of AO and its 10-alkyl derivatives into the SDS micelle consists of a rapid initial adsorption of the dye on the micelle surface and two sequential isomerization steps; one is the reorientation of the dye at the micelle surface and the other is the migration of its alkyl chain into the inner hydrophobic region of the micelle.

References

1) J. H. Fendler and E. J. Fendler, "Catalysis in Micellar and Macromolecular Systems," Academic Press, New York (1975).

2) J. H. Fendler, "Membrane Mimetic Chemistry,"

Wiley, New York (1982).
3) J. H. Fendler, *Ann. Rev. Phys. Chem.*, **35**, 137 (1984).
4) M. A. Chaiko, R. Nagarajan, and E. Ruckenstein, *J. Colloid Interface Sci.*, **99**, 168 (1984).
5) N. Ramnath, V. Ramesh, and V. Ramamurthy, *J. Photochem.*, **31**, 75 (1985).
6) Y. Chevalier and C. Chachaty, *J. Phys. Chem.*, **89**, 875 (1985).
7) J. F. Ellena, R. Dominay, and D. S. Cafiso, *J. Phys. Chem.*, **91**, 131 (1987).
8) M. F. Ottaviani, P. Baglioni, and G. Martini, *J. Phys. Chem.*, **87**, 3146 (1983).
9) Y. Kubota, M. Kodama, and M. Miura, *Bull. Chem. Soc. Jpn.*, **46**, 100 (1973).
10) H. C. Chiang and A. Lukton, *J. Phys. Chem.*, **79**, 1935 (1975).
11) W. R. Reed, M. J. Politi, and J. H. Fendler, *J. Am. Chem. Soc.*, **103**, 4591 (1981).
12) E. Blatt and W. H. Sawyer, *Biochim. Biophys. Acta*, **822**, 43 (1985).
13) A. Malliaris, *Adv. Colloid Interface Sci.*, **27**, 153 (1987).
14) K. Takeda, N. Tatsumoto, and T. Yasunaga, *J. Colloid Interface Sci.*, **47**, 128 (1974).
15) H. Hoffmann, in "Chemical and Biological Applications of Relaxation Spectroscopy," ed by E. Wyn-Jones, Reidel, Dordrecht (1975), pp. 181—193.
16) B. H. Robinson, N. C. White, and C. Mateo, *Adv. Mol. Relaxation Processes*, **7**, 321 (1975).
17) A. D. James and B. H. Robinson, *Adv. Mol. Relaxation Processes*, **8**, 287 (1976).
18) A. D. James, B. H. Robinson, and N. C. White, *J. Colloid Interface Sci.*, **59**, 328 (1977).
19) Y. Miyashita and S. Hayano, *Bull. Chem. Soc. Jpn.*, **54**, 3249 (1981).
20) E. Miethke and V. Zanker, *Z. Phys. Chem. (Frankfurt am Main)*, **18**, 375 (1958).
21) B. Tonomura, H. Nakatani, M. Ohnishi, J. Yamaguchi-Ito, and K. Hiromi, *Anal. Biochem.*, **84**, 370 (1978).
22) P. R. Bevington, "Data Reduction and Error Analysis for the Physical Sciences," McGraw-Hill, New York (1969), pp. 187—246.
23) A. Yamagishi, *J. Colloid Interface Sci.*, **81**, 511 (1981).
24) P. Mukerjee and K. J. Mysels, *J. Am. Chem. Soc.*, **77**, 2937 (1955).
25) V. Zanker, *Z. Phys. Chem. (Leipzig)*, **199**, 225 (1952).
26) K. Murakami, K. Mizuguchi, Y. Kubota, and Y. Fujisaki, *Bull. Chem. Soc. Jpn.*, **59**, 3393 (1986).
27) K. J. Mysels and L. H. Princen, *J. Phys. Chem.*, **63**, 1696 (1959).
28) K. Hiromi, "Kinetics of Fast Enzyme Reactions," Halsted Press, New York (1979), Chap. 6.
29) C. Tanford, "The Hydrophobic Effect," 2nd ed, Wiley-Interscience, New York (1980), pp. 60—78.
30) J. A. Zoltewicz and S. Munoz, *J. Phys. Chem.*, **90**, 5820 (1986).